J Appl Electrochem (2011) 41:909–917
DOI 10.1007/s10800-011-0316-x

ORIGINAL PAPER

A novel zeolite-multiwalled carbon nanotube composite for the electroanalysis of copper(II) ion

S. Senthilkumar · R. Saraswathi

Received: 14 May 2010 / Accepted: 18 April 2011 / Published online: 1 May 2011

Abstract The application of zeolite Y-multiwalled carbon nanotube (MWCNT) nanocomposite modified glassy carbon electrode (zeolite Y-MWCNT/GCE) in the electroanalysis of Cu^{2+} ion is presented. In order to bring out the unique advantage of the zeolite Y-MWCNT/GCE, experiments were carried out also at graphite/GCE, MWCNT/GCE and zeolite Y-graphite/GCE. For the same surface area, the performance of zeolite Y-MWCNT/GCE was superior to the other modified electrodes in terms of current sensitivity for Cu^{2+} ion. The combination of zeolite Y and MWCNT as a nanocomposite resulted in a good synergetic effect. The Cu^{+2} ion sensor exhibited a linear calibration range between 5×10^{-8} and 1×10^{-5} mol L^{-1} with a detection limit of 1.12×10^{-8} mol L^{-1} (0.72 ppb).

Keywords Zeolite-multiwalled carbon nanotube composite · Zeolite-modified electrode · Copper ion sensor · Synergetic effect

1 Introduction

Zeolites possess unique characteristics viz. size and shape selectivity, cation exchange capacity and catalytic effects imparted by the acidic sites in the framework which make them of immense interest in the field of electroanalytical chemistry [1]. Due to the microcrystalline nature of zeolites, special efforts are often necessary in the preparation of zeolite-modified electrodes (ZME). A common configuration is the zeolite-modified carbon paste electrode (ZMCPE) prepared with a mixture of zeolite and graphite in the presence of a binder like polystyrene or mineral oil [2, 3]. The ZMCPE has been successfully applied in several electroanalytical and electrocatalytic applications [4–7].

The use of carbon nanotubes (CNT) as an electrode material in several electrochemical applications like batteries, supercapacitors, biosensors, and electrocatalysis has been extensively reported [8–15]. CNT has also been combined with several other functional materials like metal nanoparticles, quantum dots, ceramics, and conducting polymers to form nanocomposites with either enhanced or new application prospects [16–20].

Herein, we report the electroanalytical application of a novel zeolite Y-multiwalled carbon nanotube (MWCNT) nanocomposite with Cu^{2+} ion as the chosen analyte. Zeolites being cation exchangeable are highly suitable for the detection of metal ions. The preconcentration of the analyte Cu^{+2} ions within the zeolite can lead to a several-fold enhancement in the electrochemical reduction current which will in turn help in improving the detection limit. The replacement of graphite by MWCNT in the ZME can not only be expected to impart enhanced conductivity, surface area and robustness to the ZME but rather the MWCNT can act as an active component in the electroanalysis of Cu^{2+} ion owing to its good cation adsorption capacity after acid oxidation [21]. The present study reveals a good synergy between the cation exchangeable zeolite and the metal ion adsorptive MWCNT leading to a high sensitivity in the detection of Cu^{2+} ion. Parallel experiments with plain glassy carbon electrode (GCE), MWCNT-modified GCE (MWCNT/GCE), graphite-modified GCE (graphite/GCE) and zeolite-graphite composite modified GCE (zeolite Y-graphite/GCE) have been carried out to exemplify the synergetic effect.

S. Senthilkumar · R. Saraswathi (✉)
Department of Materials Science, School of Chemistry, Madurai Kamaraj University, Madurai 625 021, Tamil nadu, India
e-mail: saraswathir@yahoo.com

2 Experimental

2.1 Materials

A commercial sample of zeolite NH_4-Y (Aldrich) was used. The molecular formula of the zeolite along with details of ion-exchangeable sites, pore size and Si/Al ratio [22] are given in Table 1. The cation exchange capacity value was estimated from the unit cell molecular weight and the number of exchangeable ions of the respective zeolite in terms of equivalents of exchangeable cations per gram. MWCNT (diameter = 10–20 nm; length = 0.5–200 μM) (Aldrich) and graphite powder (S.D's) were used after chemical oxidation using a mixture of sulfuric and nitric acids (Qualigens). Analytical grade samples of potassium ferricyanide (Aldrich), potassium nitrate (S.D's), sodium sulfate (SRL), potassium chloride (Aldrich) and anhydrous cupric chloride (S.D's) were used as received. Acetic acid (S.D's) and sodium acetate (S.D's) were used in the preparation of acetate buffer. All electrolyte solutions were prepared using high purity water with a measured resistivity of 18 MΩ cm.

2.2 Chemical oxidation of MWCNT and graphite

MWCNT and graphite were chemically oxidized with a mixture of concentrated nitric and sulphuric acids in a ratio of 1:3 [23]. MWCNT (50 mg) or graphite (50 mg) was added to 24 mL of the acid mixture in a round bottom flask, and then refluxed for 5 h. After cooling, the mixture was washed using a copious amount of double-distilled water on a Millipore polycarbonate membrane filter (0.2 μ GTTP) until the washings showed no acidity. The acid-treated sample of MWCNT or graphite could be readily dispersed in water by mild sonication.

2.3 Instrumentation and measurements

The morphological data were obtained using a scanning electron microscope (JEOL, JSM-6390, Japan). The materials coated on GCE surface were pressed onto a scotch tape and then sputter-coated with gold for imaging. The electrochemical experiments were carried out using a potentiostat/galvanostat (EG&G Model 263A, USA). A one compartment cell with provision for three electrodes was used. The GCE (3 mm diameter; CH Instruments, USA) was polished with fine alumina powder (Alfa Aesar) to a mirror finish and then thoroughly rinsed with double-distilled water. The reference electrode was a saturated calomel electrode (SCE) (pH Products, India). A large Pt foil was used as the counter electrode. 0.1 mol L^{-1} potassium chloride, 0.1 mol L^{-1} potassium nitrate, 0.1 mol L^{-1} sodium sulfate, and 0.1 mol L^{-1} acetate buffer (pH 4.2) were the electrolytes used. All the electrochemical experiments were carried out under deoxygenated condition at room temperature.

2.4 Preparation of modified electrodes

The zeolite Y-MWCNT/GCE was prepared as follows: zeolite Y (5 mg) was first dispersed in 0.5 mL double-distilled water by sonication in an ultrasonic bath for 15 min. Similarly, the acid-treated MWCNT (2.5 mg) was dispersed in 0.5 mL double-distilled water. 10 μL each of the zeolite Y and MWCNT dispersions were then mixed together in a micropipette vial from which 6 μL was cast on the polished GCE and dried in air at room temperature. The same procedure was followed in the preparation of zeolite Y-graphite/GCE by taking 2.5 mg acid-treated graphite instead of MWCNT.

The MWCNT/GCE and graphite/GCE were prepared by casting 6 μL of their dispersions on the GCE. The true surface area values of GCE and the four modified electrodes were determined from the cyclic voltammetric data for the reduction of 5×10^{-3} mol L^{-1} $K_3[Fe(CN)_6]$ in 0.1 mol L^{-1} KCl, assuming a diffusion coefficient value of 6.3×10^{-6} cm^2 s^{-1} for $K_3[Fe(CN)_6]$ [24]. The calculated true surface area values were 0.07 ± 0.003 cm^2 which was very close to the geometric area of GCE.

For the electrochemical determination of Cu^{2+} ion, the modified electrodes were immersed in a known concentration of $CuCl_2$ solution at open circuit for 20 min and then rinsed with distilled water. The preconcentrated electrode was then transferred to the electrochemical cell containing the electrolyte for voltammetric measurement.

3 Results and discussion

3.1 Morphological characterization of modified surfaces

Figure 1 shows the scanning electron microscopy (SEM) images of zeolite NH_4-Y and the four modified

Table 1 Characteristics of zeolite NH_4-Y

Zeolite name	Framework type	Composition	Si/Al ratio	Ion-exchange capacity (meq/g)	No. of exchangeable sites	Exchangeable ion	Pore size (Å)
Zeolite NH_4-Y	FAU	$Na_5(NH_4)_{46}Al_{51}Si_{141}O_{384}\cdot 250\ H_2O$	2.8	4.10	5	NH_4^+	7.4

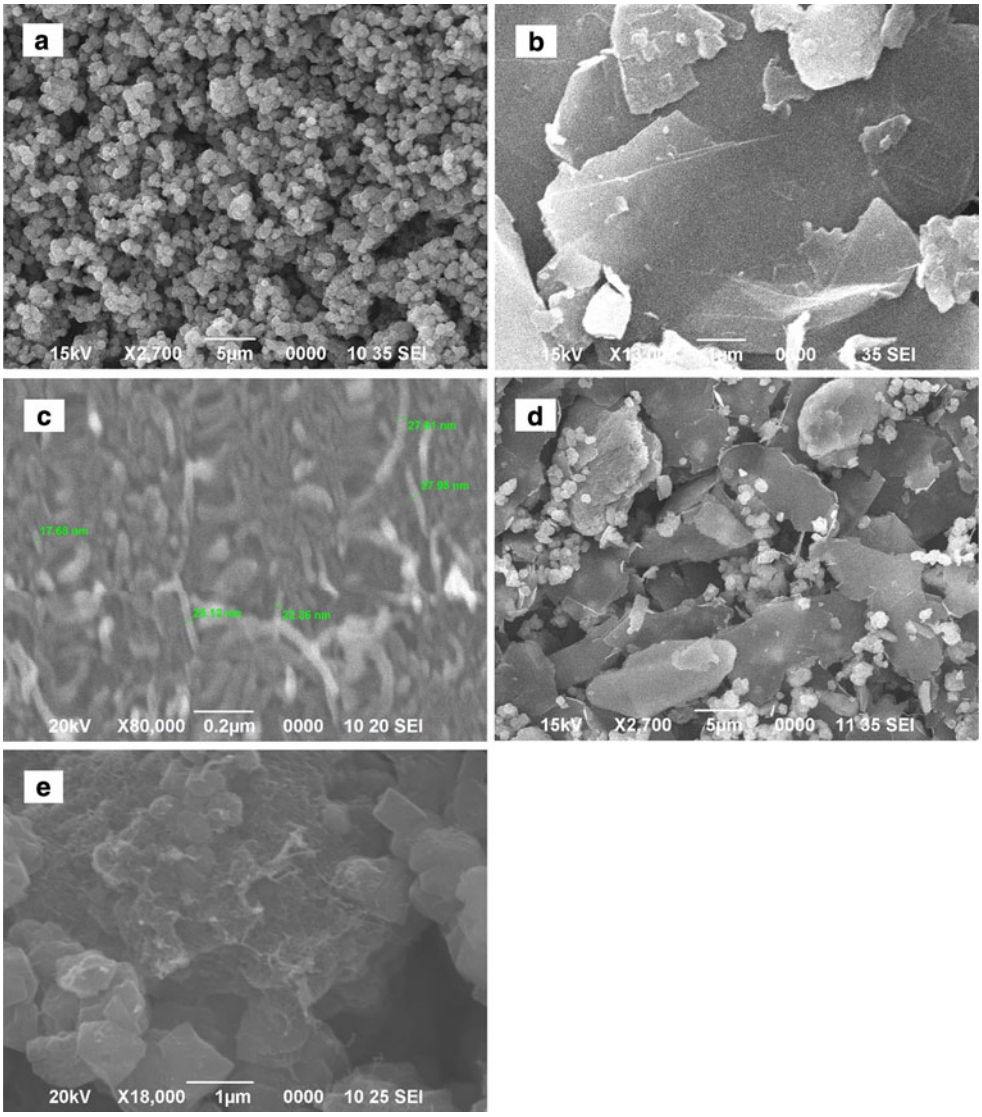

Fig. 1 Scanning electron microscopy images of **a** zeolite NH_4-Y, **b** graphite, **c** MWCNT, **d** zeolite Y-graphite, and **e** zeolite Y-MWCNT

electrode surfaces viz. graphite/GCE, MWCNT/GCE, zeolite Y-graphite/GCE and zeolite Y-MWCNT/GCE. In Fig. 1a, uniform zeolite crystals of size about 1 μm can be noticed. The graphite modified surface contained large, irregularly shaped graphite domains with random orientation and size distribution (Fig. 1b). On the other hand, the MWCNT modified surface showed a uniform distribution of nanotubes of about 20 nm diameter on the electrode surface (Fig. 1c). The SEM image of the zeolite Y-graphite composite showed a random dispersion of zeolite crystals in the carbon matrix (Fig. 1d) while that of the zeolite Y-MWCNT nanocomposite clearly indicated a well integrated and smooth morphology with the MWCNT embedded into the zeolite matrix (Fig. 1e).

3.2 Synergetic performance of zeolite Y-MWCNT/GCE

In order to bring out the unique advantages of zeolite Y-MWCNT/GCE, cyclic voltammetric experiments were carried out in 0.1 mol L^{-1} KCl at the graphite/GCE, MWCNT/GCE and zeolite Y-graphite/GCE.

Figure 2 shows the cyclic voltammograms for the reduction of Cu^{2+} at the four modified electrodes after preconcentration in 1×10^{-3} mol L^{-1} $CuCl_2$ solution for 20 min. At both graphite/GCE and MWCNT/GCE, the voltammetric peaks were found to be somewhat distorted whereas at zeolite Y-graphite/GCE and zeolite Y-MWCNT/GCE, two well-defined redox couples were

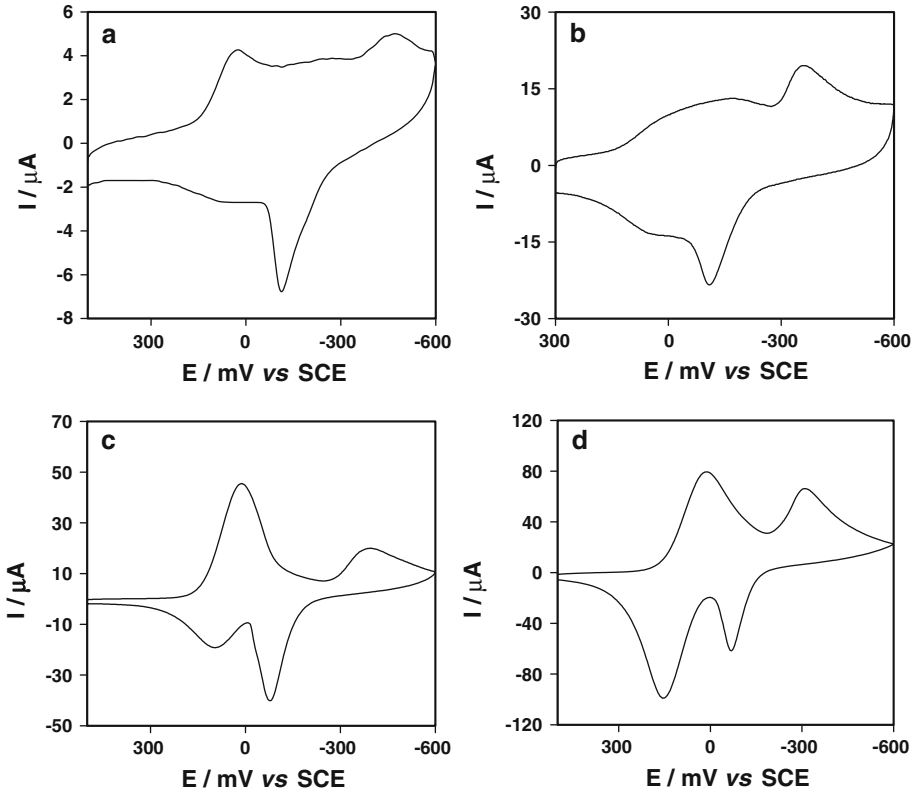

Fig. 2 Cyclic voltammograms for the reduction of Cu^{2+} (1×10^{-3} M) at **a** graphite/GCE, **b** MWCNT/GCE, **c** zeolite Y-graphite/GCE, and **d** zeolite Y-MWCNT/GCE. Supporting electrolyte: 0.1 M KCl, scan rate: 0.02 V s^{-1}, preconcentration time: 20 min

Table 2 Cyclic voltammetry data for Cu^{2+} at the four modified electrodes

Electrode	Peak potential (mV)				Peak current (μA)			
	$E_{pc(1)}$	$E_{pa(1)}$	$E_{pc(2)}$	$E_{pa(2)}$	$I_{pc(1)}$	$I_{pa(1)}$	$I_{pc(2)}$	$I_{pa(2)}$
Graphite/GCE	25	102	−467	−110	3.2	0.8	1.3	4.5
MWCNT/GCE	−16	40	−360	−120	11.3	7.0	8.3	16.3
Zeolite Y-graphite/GCE	12	118	−394	−79	42.8	14.3	12.9	37.9
Zeolite Y-MWCNT/GCE	10	153	−301	−68	76.5	83.0	36.0	63.0

The electrodes are preconcentrated in 1×10^{-3} M $CuCl_2$ for 20 min

observed. The peak potential and peak current data observed at the four modified electrodes are given in Table 2. The first redox process was more reversible than the second one. Among the four modified electrodes, zeolite Y-MWCNT/GCE showed the highest current magnitudes for all the four peaks viz. first cathodic peak ($I_{pc(1)}$), second cathodic peak ($I_{pc(2)}$), first anodic peak ($I_{pa(1)}$) and second anodic peak ($I_{pa(2)}$). The first cathodic peak was chosen as the reference to evaluate the electrode performance with respect to Cu^{2+} ion. $I_{pc(1)}$ was found to be nearly four times higher for MWCNT/GCE than for graphite/GCE. Likewise, the $I_{pc(1)}$ value at zeolite Y-MWCNT/GCE was about 7 times larger than that at MWCNT/GCE, and two times larger than that at zeolite Y-graphite/GCE (Table 2). These results clearly demonstrated the predominant role of zeolite Y-MWCNT nanocomposite in the determination of Cu^{2+} ion. The combination of zeolite Y with MWCNT as a nanocomposite resulted in a good synergetic effect in the determination of Cu^{2+} ion.

In order to bring out the significance of the Cu^{2+} ion exchange in zeolite Y in the current enhancement, direct experiments without any preconcentration were carried out at the four modified electrodes in 0.1 mol L^{-1} KCl containing 1×10^{-3} mol L^{-1} of $CuCl_2$ and the cyclic voltammograms are shown in Fig. 3. The peak potential and current data are given in Table 3. All the four modified electrodes showed two redox processes as observed with preconcentrated electrodes. Here again, the first redox process was observed to be more reversible than the second one at all the four electrodes. A comparison of the $I_{pc(1)}$ values at graphite/GCE and MWCNT/GCE in Table 3 with the corresponding data in Table 2 suggested that the uptake of Cu^{+2} ion on preconcentration in 1×10^{-3} mol L^{-1} of $CuCl_2$ for 20 min was only one-third at graphite/GCE and one-half at MWCNT/GCE. On the other hand, the 7 to

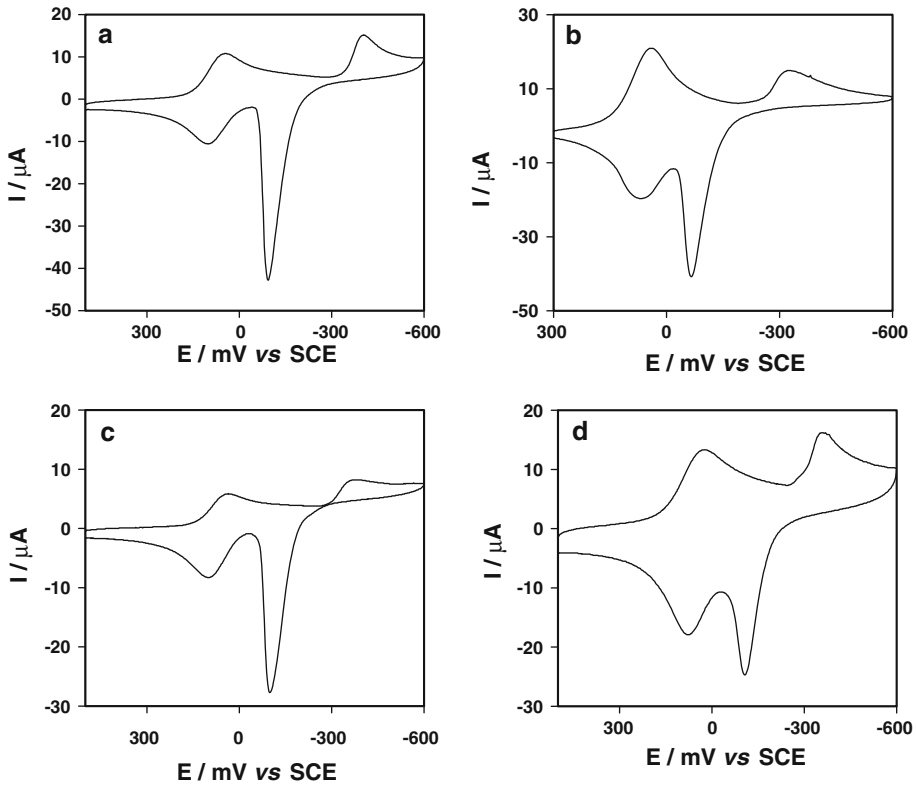

Fig. 3 Cyclic voltammograms for the reduction of Cu^{2+} (1×10^{-3} M) (without preconcentration) in 0.1 M KCl at **a** graphite/GCE, **b** MWCNT/GCE, **c** zeolite Y-graphite/GCE, and **d** zeolite Y-MWCNT/GCE. Scan rate: 0.02 V s^{-1}

Table 3 Cyclic voltammetry data for the reduction of 1×10^{-3} M $CuCl_2$ in 0.1 M KCl at the four modified electrodes

Electrode	Peak potential (mV)				Peak current (μA)			
	$E_{pc(1)}$	$E_{pa(1)}$	$E_{pc(2)}$	$E_{pa(2)}$	$I_{pc(1)}$	$I_{pa(1)}$	$I_{pc(2)}$	$I_{pa(2)}$
Graphite/GCE	47	101	−404	−94	9.9	8.2	10.1	41.1
MWCNT/GCE	10	98	−338	−77	19.1	10.7	8.4	44.0
Zeolite Y-graphite/GCE	36	97	−367	−99	5.3	7.3	4.5	26.8
Zeolite Y-MWCNT/GCE	31	73	−355	−107	10.5	11.4	8.8	24.4

8-fold enhancement in $I_{pc(1)}$ at the preconcentrated zeolite Y-graphite/GCE and zeolite Y-MWCNT/GCE compared to the respective values observed in the direct experiments clearly indicate the importance of ion exchange in zeolite Y in enhancing the current sensitivity to Cu^{2+} several-fold. Consolidating the above results, the preconcentrated zeolite Y-MWCNT/GCE is inferred to show a superior performance in the determination of Cu^{2+} among the four modified electrodes investigated.

3.3 Reduction of Cu^{2+} ion: electrolyte dependence

The reduction of Cu^{2+} was reported to be sensitive to the anion present in the electrolyte [25, 26]. The reduction occurred in two one-electron steps in ClO_4^- and Cl^- containing electrolytes owing to the stabilization of Cu^+ species by the formation of its complex ($[CuX_2]^-$) where X was the anion. When the electrolyte contained NO_3^- ions, a single two-electron reversible process was observed. Li and Calzaferri [27] observed the appearance of two redox couples in the cyclic voltammogram of copper-zeolite-modified electrode in 0.1 mol L^{-1} NaCl solution but in 0.1 mol L^{-1} $NaNO_3$, the voltammogram exhibited two close cathodic peaks with one anodic peak.

In the present study, the cyclic voltammograms of the Cu^{2+} ion-exchanged zeolite Y-MWCNT/GCE in various electrolytes including 0.1 mol L^{-1} KCl, 0.1 mol L^{-1} KNO_3, 0.1 mol L^{-1} Na_2SO_4 and acetate buffer (pH 4.2) were obtained (Fig. 4). It is clear that only in 0.1 mol L^{-1} KCl, two distinct redox processes occurred which are due to the reduction of Cu^{+2} ion occurring as two one-electron processes [25–27]. The stabilization of Cu^+ can be attributed to the formation of $[CuCl_2]^-$ complex species [28, 29]. The anion effects on the reduction of Cu^{+2} ion from the Cu^{2+} ion-exchanged zeolite Y-MWCNT/GCE suggest that the charge-transfer pathway is possibly via extrazeolite

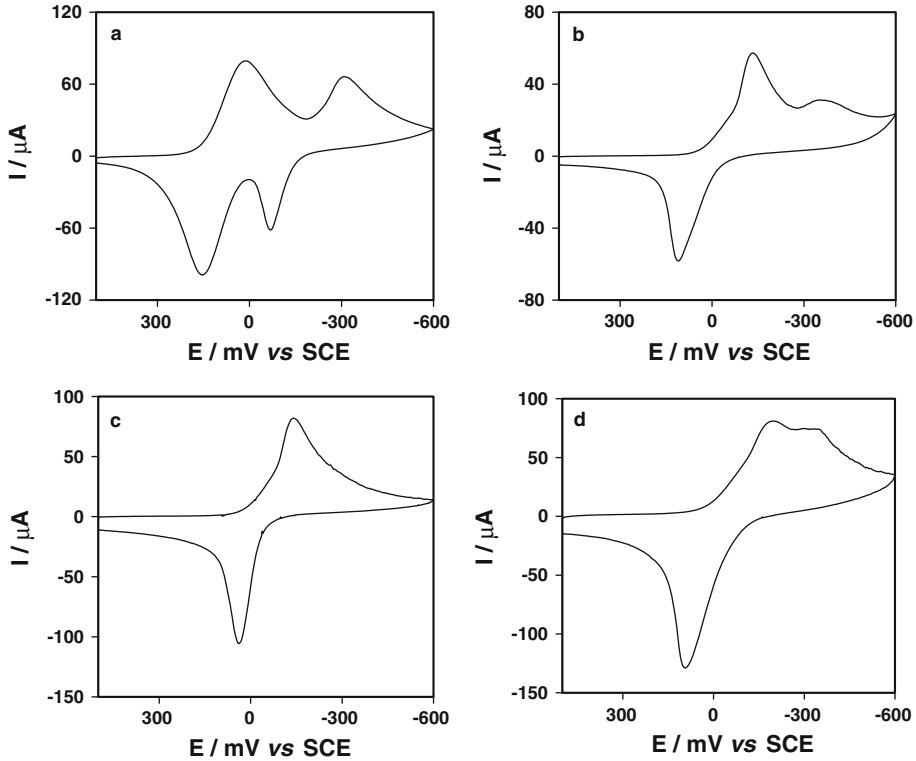

Fig. 4 Cyclic voltammograms for the reduction of Cu^{2+} (1×10^{-3} M) using a preconcentrated zeolite Y-MWCNT/GCE in **a** 0.1 M KCl, **b** 0.1 M KNO_3, **c** 0.1 M Na_2SO_4, and **d** 0.1 M Acetate buffer (pH = 4.2). Scan rate: 0.02 V s^{-1} and Preconcentration time: 20 min

electron transfer mechanism [30]. The stabilization of Cu^{+} by the anion can not happen within the zeolite due to the repulsion of the anion by the zeolite framework. Scheme 1 explains the charge and electron transfer reactions occurring at the external surface of the zeolite.

$$Cu_{Z}^{2+} + 2K_{S}^{+} \rightleftharpoons Cu_{ZM-S}^{2+} + 2K_{Z}^{+} \quad \text{(i)}$$

$$Cu_{ZM-S}^{2+} \underset{-e^-}{\overset{+e^-}{\rightleftharpoons}} Cu_{ZM-S}^{+} \underset{-2Cl^-}{\overset{+2Cl^-}{\rightleftharpoons}} [CuCl_2]_{ZM-S}^{-} \quad \text{(ii)}$$

$$Cu_{ZM-S}^{+} \underset{-e^-}{\overset{+e^-}{\rightleftharpoons}} Cu_{ZM-S}^{0} \quad \text{(iii)}$$

Scheme 1 Electron transport mechanism for the reduction of Cu^{+2} in ZME; Subscripts "Z", "S", and "ZM-S" denote "bulk zeolite", "solution phase" and "zeolite/MWCNT-solution interface", respectively

3.4 Sensor calibration

Square wave voltammetric experiments were performed in the potential range from +350 to −150 mV using the following optimal parameters: pulse height—20 mV, pulse width—2 mV, and frequency—10 Hz. The sensor calibration was made with respect to the first cathodic peak. Figure 5 shows the square wave voltammograms obtained at the zeolite Y-MWCNT/GCE in 0.1 mol L^{-1} KCl after preconcentration in the respective $CuCl_2$ analyte solution for a period of 20 min. The analyte concentration was in the range between 5×10^{-8} and 1×10^{-5} mol L^{-1}. The peak potential value was nearly the same at all concentrations. The sensor calibration plot is shown in Fig. 6. A linear response was observed in the concentration range between 5×10^{-8} and 1×10^{-5} mol L^{-1} with the slope and regression coefficient values of 1.69 μA μM^{-1} and 0.99, respectively. The detection limit was calculated using the Eq. 1 [31]:

$$\text{Detection Limit} = \frac{3 \times S}{N} \quad (1)$$

where S is the standard deviation of the repeat measurements at the lowest detectable concentration and N is the slope of the calibration plot. The signal-to-noise ratio is the ratio between the mean value of repeat measurements and its standard deviation. In order to find the detection limit of Cu^{2+}, five repeat measurements were carried out at the lowest concentration of 5×10^{-8} mol L^{-1} (standard deviation: 0.006 μA). The detection limit was then calculated to be 1×10^{-8} mol L^{-1} (0.72 ppb) with a signal-to-noise ratio of 23.

The earlier attempts in developing an electrochemical sensor for Cu^{2+} ion based on ZMCPE resulted in a detection limit as low as 0.95 ppb with a linear calibration range from 5×10^{-8} to 5×10^{-6} mol L^{-1} using the natural zeolite clinoptilolite in 0.05 mol L^{-1} $NaNO_3$ [32]. Zeolites X, Y and 13X were also investigated for the determination of Cu^{2+} ion [33–37]. Walcarius et al. [35]

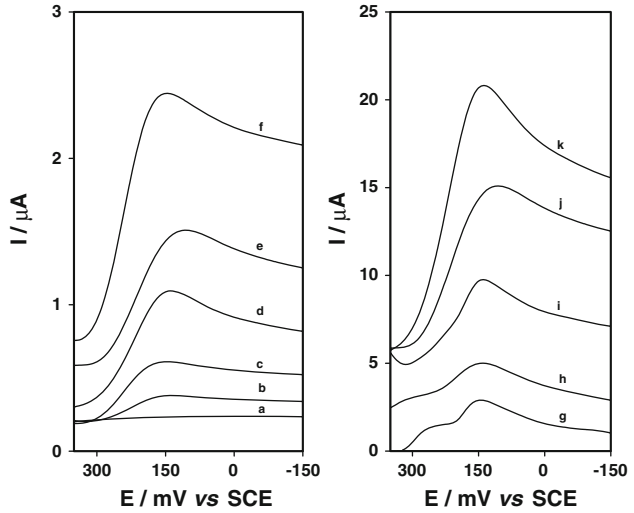

Fig. 5 Square wave voltammograms for various concentrations of Cu^{2+} at zeolite Y-MWCNT/GCE (for clarity voltammograms are grouped in two separate figures). Curve (*a*) is the background response. The concentrations of Cu^{2+}: (*b*) 5×10^{-8}, (*c*) 1×10^{-7}, (*d*) 2.5×10^{-7}, (*e*) 5×10^{-7}, (*f*) 7.5×10^{-7}, (*g*) 1×10^{-6}, *h* 2.5×10^{-6}, (*i*) 5×10^{-6}, (*j*) 7.5×10^{-6}, and (*k*) 1×10^{-5} M. Supporting electrolyte: 0.1 M KCl and preconcentration time: 20 min. SWV parameters: pulse height: 20 mV, pulse width: 2 mV and frequency: 10 Hz

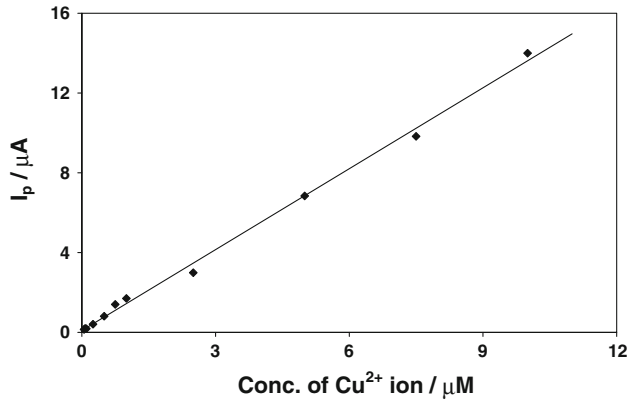

Fig. 6 Sensor calibration curve for the square wave voltammetry detection of Cu^{2+} at zeolite Y-MWCNT/GCE. Concentration range: 5×10^{-8}–1×10^{-5} M

showed that between ZMCPE and zeolite monograin layers coated on GCE, the former presented a better current response to Cu^{2+} ion. In another study, the authors reported that the ZMCPE prepared with solid paraffin as binder exhibited superior electrochemical performance than that made with silicone oil as binder in the determination of Cu^{2+} ion [36]. The Cu^{2+} ion sensor data at various ZMEs are compiled in Table 4 for comparison with the present study. It can be inferred that the zeolite Y-MWCNT/GCE used in this study gives a wider linear calibration range along with a slightly better detection limit of 0.72 ppb.

Table 4 Reported details of the detection of Cu^{2+} at various ZMEs for comparison with present study

Material	Medium	Technique	Concentration range/M	Detection limit/ppb	Ref.
Zeolite 13X-graphite with silicone oil as binder	Ammonia buffer (pH 9)	SWV	5.0×10^{-6}–1.5×10^{-5}	19.0	[33]
Zeolite 13X-graphite with silicone oil as binder	Phosphate buffer (pH 4.2)	SWV	5.0×10^{-6}–1.5×10^{-5}	74.0	[34]
Clinoptilolite-graphite with mineral oil as binder	0.05 M $NaNO_3$	DPV	5.0×10^{-8}–5.0×10^{-6}	0.95	[32]
Zeolite X-graphite with silicone oil as binder	Phosphate buffer (pH 3.7)	SWV	1.0×10^{-6}–1.0×10^{-3}	50.0	[37]
Zeolite Y-MWCNT	0.1 M KCl	SWV	5.0×10^{-8}–1.0×10^{-5}	0.72	Present study

SWV square wave voltammetry, *DPV* differential pulse voltammetry

3.5 Interference studies: effects of alkali metal ions

The alkali metal ions such as Li^+, Na^+, and K^+ were selected for interference studies. The analyte concentration was fixed at 1×10^{-3} mol L^{-1}. The concentrations of interfering alkali metal ions were 5.0×10^{-6}, 1.0×10^{-5}, 5.0×10^{-5}, 1.0×10^{-4}, and 1.5×10^{-4} mol L^{-1}. The zeolite Y-MWCNT/GCE was preconcentrated for 20 min in a solution containing both Cu^{2+} and Li^+ or Na^+ or K^+ ions before doing the voltammetry experiment in 0.1 mol L^{-1} KCl. Figure 7 shows the $I_{pc(1)}$ observed for the reduction of Cu^{2+} against the concentration of the interfering ion. It can be found that as the concentration of the interfering ion increased, the $I_{pc(1)}$ value increased to some extent for Li^+, whereas it decreased for both Na^+ and K^+ ions. The increase in $I_{pc(1)}$ of Cu^{2+} on ion exchange with Li^+ is unexpected. The Li^+ ion exchange in zeolite Y was found to be a very slow and non-spontaneous process due to a large standard Gibbs energy value of 2,860 cal g^{-1} $equiv^{-1}$ [22]. In our earlier study, a somewhat similar observation of an increase in the tetraethylammonium ion transfer current across the zeolite-modified interface between two immiscible electrolyte solutions was noticed on ion exchange with Li^+ at concentrations less than 5×10^{-3} mol L^{-1} which was attributed to an increase in transport rate of tetraethylammonium ion [38]. The decrease in peak current in the presence of Na^+ and K^+ can be attributed to the competitive ion exchange between Cu^{2+} and the interfering alkali metal ions [27]. Between Na^+ and K^+ ions, the interference due to the K^+ ion is more than that of Na^+ ion which can be attributed to the relative ease of ion exchange due to the lower value of the radius of the hydrated K^+ ion (3.31 Å) compared to that of Na^+ ion (3.58 Å) [39].

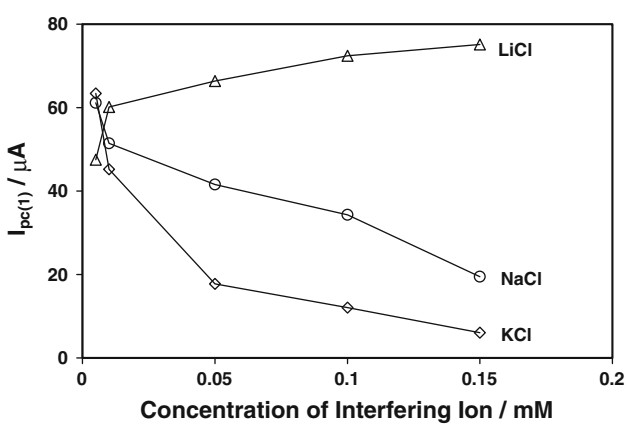

Fig. 7 Plots of first cathodic peak current ($I_{pc(1)}$) for the detection of Cu^{2+} at zeolite Y-MWCNT/GCE against the concentration of interfering ions. The electrode has been preconcentrated for 20 min in a solution containing Cu^{2+} and Li^+ or Na^+ or K^+ ions before doing experiment in 0.1 M KCl

4 Conclusion

A novel zeolite Y-MWCNT nanocomposite-modified electrode was developed as a sensor electrode for the detection of Cu^{2+} ion. The use of binding material was avoided in the preparation of zeolite Y-MWCNT/GCE. The enhanced current sensitivity at the nanocomposite electrode suggested a good synergetic effect between zeolite Y and MWCNT. The application of square wave voltammetry led to a detection limit of 0.72 ppb with a linear calibration range between 5×10^{-8} and 1×10^{-5} mol L^{-1}.

Acknowledgments SS thanks the Council of Scientific and Industrial Research, New Delhi for the award of a Senior Research Fellowship. RS acknowledges the financial assistance from the Department of Science and Technology, New Delhi and under the University with Potential for Excellence scheme from the University Grants Commission, New Delhi.

References

1. Walcarius A (2003) In: Auerbach SM, Karrado KA, Dutta PK (eds) Handbook of zeolite science and technology. Marcel Dekker Inc., New York
2. Li Z, Mallouk TE (1987) J Phys Chem 91:643
3. Wang J, Martinez T (1988) Anal Chim Acta 207:95
4. Walcarius A (1996) Electroanalysis 8:971
5. Rolison DR (1990) Chem Rev 90:867
6. Rolison DR, Bassel CA (2000) Acc Chem Res 33:737
7. Walcarius A (2008) Electroanalysis 20:711
8. Ajayan PM, Zhou OZ (2001) Top Appl Phys 80:391
9. Wang J (2005) Electroanalysis 17:7
10. Trojanowicz M (2006) Trends Anal Chem 25:480
11. Kauffman DR, Star A (2008) Angew Chem Int Ed 47:6550
12. Zhang H, Cao G, Yang Y (2009) Energy Environ Sci 2:932
13. Jacobs CB, Peairs MJ, Venton BJ (2010) Anal Chim Acta 662:105
14. Lota G, Fic K, Frackowiak E (2011) Energy Environ Sci. doi: 10.1039/C0EE00470G
15. Vashist SK, Zheng D, Al-Rubeaan K, John HT, Luong JHT, Sheu FS (2011) Biotechnol Adv 29:169
16. Wildgoose GG, Banks CE, Compton RG (2006) Small 2:182
17. Haremza JM, Hahn MA, Krauss TD, Chen S, Calcines J (2002) Nano Lett 2:1253
18. Samal SS, Bal S (2008) J Min Mater Charact Eng 7:355
19. Downs C, Nugent J, Ajayan PM, Duquette DJ, Santhanam KSV (1999) Adv Mater 11:1028
20. Qian H, Greenhalgh ES, Shaffer MSP, Bismarck A (2010) J Mater Chem 20:4751
21. Li YH, Luan Z, Xiao X, Zhou X, Xu C, Wu D, Wei B (2003) Adsorpt Sci Technol 21:475
22. Breck DW (1974) Zeolite molecular sieves: structure, chemistry and use. Wiley, London
23. Shaffer MSP, Fan X, Windle AH (1998) Carbon 36:1603
24. Mo C, Zhong M, Zhong Q (2000) J Electroanal Chem 493:100
25. Štulíková M, Vydra F (1973) J Electroanal Chem 44:117
26. Baldo MA, Bragato C, Mazzocchin GA, Daniele S (1998) Electrochim Acta 43:3413
27. Li JW, Calzaferri G (1994) J Electroanal Chem 377:163
28. Gunawardena G, Hills G, Montenegro I (1985) J Electroanal Chem 184:357

29. Daniele S, Pena MJ (1993) Electrochim Acta 38:165
30. Senaratne C, Zhang J, Baker MD, Bassel CA, Rolison DR (1996) J Phys Chem 100:5849
31. Skoog DA, Holler FJ, Crouch SR (2007) Instrumental analysis. Cengage Learning, New Delhi
32. Alpat SK, Yuksel U, Akcay H (2005) Electrochem Commun 7:130
33. Bing C, Kryger L (1996) Talanta 43:153
34. Chen B, Goh NK, Chia LS (1997) Electrochim Acta 42:595
35. Walcarius A, Barbaise T, Bessière J (1997) Anal Chim Acta 340:61
36. Walcarius A, Mariaulle P, Lamberts L (2003) J Solid State Electrochem 7:671
37. Mazloum-Ardakani M, Akrami Z, Kazemian H, Zare HR (2009) Int J Electrochem Sci 4:308
38. Senthilkumar S, Dryfe RAW, Saraswathi R (2007) Langmuir 23:3455
39. Nightingale ER Jr (1959) J Phys Chem 63:1381